2009 American Control Conference
Hyatt Regency Riverfront, St. Louis, MO, USA
June 10-12, 2009

Nonlinear Robust Stochastic Control for Unmanned Aerial Vehicles

Yunjun Xu

Abstract—**Almost all dynamical systems experience inherent uncertainties such as environmental disturbance and sensor noise. This paper describes a new robust stochastic control methodology, which is capable of controlling the statistical nature of state variables of a nonlinear system to designed (attainable) statistical properties. First, an asymptotically stable and robust output tracking controller is designed in which discontinuous functions are not involved. Second, undetermined control parameters in the closed-loop system are optimized through nonlinear programming. In this constrained optimization, the error between the desired and actual moments of state variables is minimized subject to constraints on statistical moments. As the key point to overcome the difficulties in solving the associated Fokker-Planck equation, a direct quadrature method of moments is proposed. The advantages of the proposed method are: (1) ability to control any specified stationary moments of the states or output probability density function; (2) no need for the state process to be a Gaussian; (3) robustness with respect to parametric and functional uncertainties.**

I. Introduction

VIEWING system behaviors within a stochastic framework allows for the inclusion of random disturbances and calculation of expected long term system trends. Normally Monte Carlo simulation approaches are used to find proper control parameters such that a desired statistical distribution of system performance can be achieved. However, this approach has a polynomial complexity in computation [1]. It will become intractable when the system is large, which results in a prohibitive number of control design iterations and CPU and labor time. To reduce the computational cost, extensive research efforts were spent for both linear and nonlinear stochastic systems, as discussed below.

On one hand, the stochastic control for linear systems, such as LQG, observer based covariance control, optimal sliding mode regulator, and minimum energy covariance control etc., has been well studied [2-9]. On the other hand, the methods have been investigated to address nonlinear stochastic problems, which can be broadly put into three categories.

The first and the most intuitive way of handling nonlinear stochastic control problems is to linearize the system in a statistical way, after which linear stochastic control methods could be applied [10]. The shortcoming is obvious: it is expected that a linear controller will only provide a good closed-loop performance locally [11].

The second approach to solve nonlinear stochastic control problems is via the solution of the associated Fokker-Planck Equation once the structure of the closed-loop system is known. However, solving the associated Fokker-Planck Equation (FPE) [12] makes this problem cumbersome with few exceptions due to the curse of dimensionality [13]. To mitigate the computational cost, methods such as the path integral method [15], cell-mapping method [14] and adaptive grids methods [16-17] have been tried. However, the computational cost in these methodologies is still high.

Many interests have been attracted to the third category, approximation methods [11, 18-25], through which the solution of the FPE is approximated. In the present work, a novel approach is proposed, referred as the direct quadrature method of moments (DQMOM), along with an asymptotically stable nonlinear tracking control. This approach involves representing the state PDF in terms of a finite summation of Dirac delta functions, whose weights and locations (abscissas) are determined based on moments constraints. Using a small number of scalars, the method is able to efficiently and accurately model stochastic processes described by the multidimensional FPE through a set of ordinary differential equations (ODEs). Together with the DQMOM approach, a nonlinear controller is designed here based on the concepts of sliding manifold and input-output feedback linearization with guaranteed asymptotic tracking stability. Different from the commonly used sliding mode control (SMC) [26-29], the high speed switching (discontinuous) function shown in typical SMCs or higher order SMCs has been removed to satisfy the continuity requirement in the partial derivatives of the associated FPE. In addition, the inherent chattering problem experienced in the commonly used SMC can be eliminated.

The main contributions of the paper can be summarized as follows. First, the existence of a finite moment index implies that the controlled system is stable up to the highest order of statistical moments included in the off-line design. Second, selected moments of the state or output variables can be controlled accurately in steady state and the state process doesn't need to be a Gaussian. Third, the nonlinear controller proposed here is asymptotically stable and robust to bounded parametric as well as functional uncertainties.

The rest of this paper is organized as follows. First, the system model of an affine nonlinear stochastic system is described along with the control objectives and the nominal system used in the design stage. Second, the governing equations of the weights and abscissas, which are used in

Y. Xu is with the Department of Mechanical, Materials, and Aerospace Engineering, University of Central Florida, Orlando, FL 32816 USA. Phone: 407-823-1745; Fax: 407-823-0208; (e-mail: yjxu@ou.edu).

978-1-4244-4524-0/09/$25.00 ©2009 AACC

representing the state PDF, are derived for the FPE based upon the proposed quadrature based moment approach. Third, a nonlinear robust control method is proposed based on the concepts of input-output feedback linearization and sliding manifold without involving discontinuous functions. Next, the undetermined control parameters, weights and abscissas are optimized offline through a constrained nonlinear optimization. Finally, a non-trivial numerical example is illustrated, followed by the conclusion.

II. The System Model and Control Objectives

Let us consider the following control-affine nonlinear stochastic differential equation (SDE) with additive noise

$$x_i^{(n_i)} = f_i(\boldsymbol{x}_1,...,\boldsymbol{x}_n,t) + \sum_{j=1}^{m} b_{ij}(\boldsymbol{x}_1,...,\boldsymbol{x}_n)u_j + \sum_{j=1}^{N_w} g_{ij}(\boldsymbol{x}_1,...,\boldsymbol{x}_n)w_j(t),\ i=1,...,n \quad (1)$$

and an output model to be

$$y_i = h_i(\boldsymbol{x}_1,...,\boldsymbol{x}_n),\ i=1,...,p \quad (2)$$

where $\boldsymbol{x}_i \in \Re^{n_i}$ and $x_i^{(n_i-1)} \triangleq d^{n_i-1}x_i / dt^{n_i-1}$ are states with up to $n_i - 1$ derivatives. $\boldsymbol{u} \in \Re^m$ is the control input and $\boldsymbol{B} \in \Re^{n\times m}$ and $\boldsymbol{f} \in \Re^n$ are the input matrix and state function, respectively. The relative degree of the output $\boldsymbol{y} = \boldsymbol{h} \in \Re^p$ is $\boldsymbol{r} \in \Re^p$. In this paper, only the case when $p \le m$ is considered to avoid numerical errors in the pseudo inverse associated with the proposed controller. When $p > m$, singular perturbation or multi-time scale decomposition methods can be used [30-31]. $\boldsymbol{w}(t) \in \Re^{N_w}$ is assumed to be a Weiner process [12] with a zero-mean and a covariance matrix of $\boldsymbol{Q}(t)$, and $\boldsymbol{G} = \left[g_{ij}\right] \in \Re^{n\times N_w}$ is the associated matrix.

The nonlinear robust controller is designed based on the following nominal system

$$x_i^{(n_i)} = \hat{f}_i(\boldsymbol{x}_1,...,\boldsymbol{x}_n,t) + \sum_{j=1}^{m} \hat{b}_{ij}(\boldsymbol{x}_1,...,\boldsymbol{x}_n)u_j,\ i=1,...,n \quad (3)$$

with the nominal output model as

$$y_i = \hat{h}_i(\boldsymbol{x}_1,...,\boldsymbol{x}_n),\ i=1,...,p \quad (4)$$

where $\wedge$ represents the nominal information. The parametric uncertainties of the input matrix are bounded by $|\Delta_{ij}| \le D_{ij},\ i,j=1,...,p$, in which the bounds are calculated by

$$(\boldsymbol{I}+\boldsymbol{\Delta}) = \left[L_{\boldsymbol{B}} L_{\boldsymbol{f}}^{r-1}\boldsymbol{h}(\boldsymbol{x})\right]\left[L_{\hat{\boldsymbol{B}}} L_{\hat{\boldsymbol{f}}}^{r-1}\hat{\boldsymbol{h}}(\boldsymbol{x})\right]^{+},\ \boldsymbol{\Delta} \in \Re^{p\times p} \quad (5)$$

and $\boldsymbol{I}$ is an identity matrix with a proper dimension. $\boldsymbol{B}$ and $\hat{\boldsymbol{B}}$ are assumed to satisfy the matching condition [28], i.e. the maximum eigenvalue of the matrix $\boldsymbol{D}$ satisfy $\lambda_{\max}(\boldsymbol{D}) < 1$. "$L$" and "$+$" are used to denote the Lie derivative and the pseudo inverse, respectively. The error between the nominal and actual state functions is bounded by $\boldsymbol{F} = [F_1,...,F_p]^T \in \Re^p$ as

$$F_i = \left|-L_{\boldsymbol{f}}^{r_i} h_i + L_{\hat{\boldsymbol{f}}}^{r_i} \hat{h}_i\right|,\ i=1,...,p \quad (6)$$

III. Nonlinear Stochastic Control Based Upon DQMOM

Once the feedback control law $u_j = u_j(\boldsymbol{x}_1,...,\boldsymbol{x}_n,\boldsymbol{\lambda},\boldsymbol{\eta})$, to be described in the next section, is designed, the state equation of the closed-loop SDE (Eq. 1) can be rewritten as

$$\begin{aligned} x_i^{(n_i)} &= f_i(\boldsymbol{x}_1,...,\boldsymbol{x}_n,t) + \sum_{j=1}^{m} b_{ij}(\boldsymbol{x}_1,...,\boldsymbol{x}_n)u_j(\boldsymbol{x}_1,...,\boldsymbol{x}_n,\boldsymbol{\lambda},\boldsymbol{\eta}) \\ &+ \sum_{j=1}^{N_w} g_{ij}(\boldsymbol{x}_1,...,\boldsymbol{x}_n)w_j(t),\ i=1,...,n \end{aligned} \quad (7)$$

where $\boldsymbol{\lambda}$ and $\boldsymbol{\eta}$ are the control parameters to be determined. The n_i^{th} order ODE equation (7) can be converted into the first order Itô form as

$$d\hat{x}_i = \hat{f}_i(\boldsymbol{x}_1,...,\boldsymbol{x}_n,\boldsymbol{\lambda},\boldsymbol{\eta},t)dt + \sum_{j=1}^{N_w} \hat{g}_{ij}(\boldsymbol{x}_1,...,\boldsymbol{x}_n)d\beta_j(t),\ i=1,...,N_s \quad (8)$$

where $N_s = \sum_i^n n_i$ is the number of states $\hat{x}_i$ (i.e., $\hat{\boldsymbol{x}}(t) \in \Re^{N_s}$) in the first order system. According to Jazwinski [12], $w_j(t) \sim d\beta_j(t)/dt$ and $d\beta_j(t) \sim \mathbb{N}(0,dt)$ is a normal distribution. $\hat{\boldsymbol{G}} = [\hat{g}_{ij}] \in \Re^{N_s\times N_w}$ is the associated matrix.

If the process described by the SDE (Eq. 8) is a Markovian diffusion process, the PDF characterizing this process is governed by the FPE [12] as

$$\frac{\partial p}{\partial t} = -\sum_{i=1}^{N_s}\frac{\partial\left[p\hat{f}_i\right]}{\partial\hat{x}_i} + \frac{1}{2}\sum_{i=1}^{N_s}\sum_{j=1}^{N_s}\frac{\partial^2\left[p\left(\hat{\boldsymbol{G}}\boldsymbol{Q}\hat{\boldsymbol{G}}^T\right)_{ij}\right]}{\partial\hat{x}_i\partial\hat{x}_j} \quad (9)$$

where $p = p(\hat{\boldsymbol{x}})$ is the state PDF. The first term on the right hand side (RHS) of the FPE is the drift term, whereas the second one is the diffusion term.

Here, a new quadrature based moment approach is proposed for solving the FPE efficiently. This method involves the approximation of the state PDF in terms of a finite summation of Dirac delta functions as

$$p\left(\hat{\boldsymbol{x}}(t)\right) = \sum_{\alpha=1}^{N} w_\alpha(t)\prod_{j=1}^{N_s}\delta[\hat{x}_j - \left\langle\hat{x}_j\right\rangle_\alpha] \quad (10)$$

where N is the number of nodes, $w_\alpha = w_\alpha(t)$ denotes the corresponding weight for node α, $\alpha=1,...,N$. $\left\langle\hat{x}_j\right\rangle_\alpha = \left\langle\hat{x}_j\right\rangle_\alpha(t),\ j=1,...,N_s$ represents the property vector of node α, called "abscissas" here.

Theorem 1: The dynamics of the abscissas and weights are governed by the following differential algebraic equations

$$\begin{aligned} &\sum_{\alpha=1}^{N}\left[\left(1-\sum_{j=1}^{N_s}k_j\right)\prod_{q=1}^{N_s}\left\langle\hat{x}_q\right\rangle_\alpha^{k_q}\right]a_\alpha + \sum_{\alpha=1}^{N}\sum_{j=1}^{N_s}k_j\left\langle\hat{x}_j\right\rangle_\alpha^{k_j-1}\prod_{q=1,q\ne j}^{N_s}\left\langle\hat{x}_q\right\rangle_\alpha^{k_q}b_{j\alpha} \\ &= \bar{S}_{k_1,...k_{N_s}} \end{aligned} \quad (11)$$

with the definitions of

$$dw_\alpha / dt \triangleq a_\alpha,\ \alpha=1,...,N \quad (12)$$

and

$$d\varsigma_{j\alpha} / dt \triangleq b_{j\alpha},\ j=1,...,N_s;\ \alpha=1,...,N \quad (13)$$

The weighted abscissas $\varsigma_{j\alpha} \triangleq w_\alpha\left\langle\hat{x}_j\right\rangle_\alpha$ is introduced. The moment constraint is derived as $\bar{S}_{k_1,\dots k_{N_s}} \triangleq \bar{S}^1_{k_1,\dots k_{N_s}} + \bar{S}^2_{k_1,\dots k_{N_s}}$ as

$$\begin{aligned}\bar{S}^1_{k_1,\dots k_{N_s}} = \sum_{i=1}^{N_s}\sum_{\alpha=1}^{N} k_i w_\alpha(t)\langle\hat{x}_1\rangle_\alpha^{k_1}\cdots\langle\hat{x}_{i-1}\rangle_\alpha^{k_{i-1}}\langle\hat{x}_i\rangle_\alpha^{k_i-1}\langle\hat{x}_{i+1}\rangle_\alpha^{k_{i+1}} \\ \cdots\langle\hat{x}_{N_s}\rangle_\alpha^{k_{N_s}}\hat{f}_i(\langle\hat{x}_1\rangle_\alpha,\dots\langle\hat{x}_{N_s}\rangle_\alpha)\end{aligned} \quad (14)$$

and

$$\bar{S}^2_{k_1,\dots k_{N_s}} = \begin{cases} \sum_{i=1}^{N_s}\sum_{j=1}^{N_s}\sum_{\alpha=1}^{N} w_\alpha k_i k_j \left(\prod_{q=1}^{N_s}\langle\hat{x}_q\rangle_\alpha^{k_q}\right) / \langle\hat{x}_i\rangle_\alpha\langle\hat{x}_j\rangle_\alpha [\boldsymbol{D}(\hat{x})]_{ij}\Big|_{\langle\hat{x}_1\rangle_\alpha,\dots\langle\hat{x}_{N_s}\rangle_\alpha} & i\neq j \\ \sum_{i=1}^{N_s}\sum_{i=1}^{N_s}\sum_{\alpha=1}^{N} w_\alpha k_i(k_i-1)\left(\prod_{q=1}^{N_s}\langle\hat{x}_q\rangle_\alpha^{k_q}\right) / \langle\hat{x}_i\rangle_\alpha^2[\boldsymbol{D}(\hat{x})]_{ii}\Big|_{\langle\hat{x}_1\rangle_\alpha,\dots\langle\hat{x}_{N_s}\rangle_\alpha} & i=j \end{cases} \quad (15)$$

where $\boldsymbol{D} \triangleq 1/2\hat{\boldsymbol{G}}\boldsymbol{Q}\hat{\boldsymbol{G}}^T$. The proof of Theorem 1 is shown in omitted here due to the page limit. Once the abscissas and weights are calculated, any selected statistical moment of the state PDF can be found from

$$M^{k_1k_2\dots k_{N_s}} \triangleq \sum_{\alpha=1}^{N} w_\alpha \prod_{j=1}^{N_s}\langle\hat{x}_j\rangle_\alpha^{k_j} \quad (16)$$

where $k_1,k_2,\dots,k_{N_s}$ are nonnegative integers and used to denote the $k_1,k_2,\dots,k_{N_s}$ moments of the state statistics.

Lemma 1: For any selected nonnegative integers $k_1,k_2,\dots,k_{N_s}$, the corresponding stationary moment of the PDF is by

$$\bar{S}_{k_1,\dots k_{N_s}} = 0 \quad (17)$$

Proof: In steady state, the abscissas and weights of the moments will not change in time; therefore, based on Eq. 11, the LHS is zero.

IV. Nonlinear Robust Control

In this section, a nonlinear robust controller $u_j = u_j(\boldsymbol{x}_1,\dots,\boldsymbol{x}_n,\boldsymbol{\lambda},\boldsymbol{\eta})$ will be proposed. Unlike a commonly used SMC approach [26-27], there is no discontinuous function involved. The later fact is preferred by the FPE based approach because of continuity requirements in the partial derivatives. Let us define the sliding manifold $\boldsymbol{s} = [s_1,\dots,s_p]^T \in \Re^p$ as

$$s_i = \sum_{k=0}^{r_i-2}\lambda_{k,i}e_i^{(k)} + e_i^{(r_i-1)}, i=1,\dots,p \quad (18)$$

where $\lambda_{k,i} > 0,\ k=0,\dots,r_i-2,\ i=1,\dots p$ can be any positive number and the error signal is defined as $e_i = y_{i,d} - y_i,\ i=1,\dots,p$.

<u>*Theorem 2:*</u> For a nonlinear system (Eq. 1) with bounded parametric and functional uncertainties (Eqs. 5 and 6), the proposed MIMO feedback control scheme

$$\boldsymbol{u} = \left[L_{\hat{B}}L_{\hat{f}}^{r-1}\hat{\boldsymbol{h}}(\boldsymbol{x})\right]^+\left[\frac{d^r\boldsymbol{y}_d}{dt^r} - L_{\hat{f}}^r\hat{\boldsymbol{h}}(\boldsymbol{x}) + \sum_{k=0}^{r-2}\boldsymbol{\lambda}_k\cdot\boldsymbol{e}^{(k+1)} + \boldsymbol{k}\cdot\boldsymbol{s}\right] \quad (19)$$

guarantees that the closed-loop system is globally asymptotically stable for tracking desired signal $y_{i,d}$.

<u>*Lemma 2:*</u> The time varying feedback gain $\boldsymbol{k} = [k_1,\dots,k_p]^T \in \Re^p$ can be uniquely solved from

$$\boldsymbol{F} + \boldsymbol{D}\left|\frac{d^r\boldsymbol{y}_d}{dt^r} - L_{\hat{f}}^r\hat{\boldsymbol{h}}(\boldsymbol{x}) + \sum_{k=0}^{r-2}\boldsymbol{\lambda}_k\cdot\boldsymbol{e}^{(k+1)}\right| + \boldsymbol{\eta}\cdot\boldsymbol{s} = (\boldsymbol{I}-\boldsymbol{D})\boldsymbol{k}\cdot\boldsymbol{s} \quad (20)$$

for any positive numbers $\boldsymbol{\lambda}$ and $\boldsymbol{\eta}$. In the case of $s_i \to 0$, the magnitude of k_is_i ($\varsigma_i = |k_is_i|$) instead of k_i will be calculated using Eq. (20) because the proposed controller Eq. (19) only uses k_is_i. The sign of k_is_i is determined by s_i since $k_i > 0$. The proofs of Theorem 2 and Lemma 2 are provided in [31].

V. Offline Constrained Nonlinear Optimization

The method to find proper control parameters $\boldsymbol{\lambda}$ and $\boldsymbol{\eta}$, under the constraints of nonnegative thus the asymptotically stability is guaranteed, will be illustrated here. The objective is to achieve the desired moments of the closed-loop system. The basic procedure involves the minimization of the weighted error norm between the desired moment $M_d^{k_1k_2\dots k_{N_s}}$ and actual moment $M^{k_1k_2\dots k_{N_s}}$ through nonlinear programming. The equality constraint is $\sum_{\alpha=1}^{N} w_\alpha = 1$ (property of the PDF), whereas $\boldsymbol{\eta} > 0$ (stability requirement), $\boldsymbol{\lambda} > 0$ (stability requirement), and $w_\alpha > 0$ (property of the PDF) are inequality constraints. The parameters to be optimized are control parameters $\boldsymbol{\lambda}$ and $\boldsymbol{\eta}$, the weights w_α, and the abscissas $\langle\hat{x}_j\rangle_\alpha$. Note that due to the flexibility of the NLP approach used here, the performance index can be extended to a more general form, but not limited to the quadratic type index.

VI. Numerical Simulation

The effectiveness of the proposed algorithm is demonstrated in the following non-trivial generic UAV command tracking problem. Note that although the example used here is a state feedback controller, the methodologies proposed in this paper can be extended to output feedback control, in which the actual and desired moments of output variables instead of state variables will be in the offline optimization.

A. Dynamics Model and Control Objectives

Assuming that the Earth is flat, and the fuel expenditure is negligible, i.e. the center of mass is time invariant, the UAV dynamics can be expressed in the wind system as

$$\dot{\boldsymbol{x}} = \begin{bmatrix}\dot{V}\\ \dot{\gamma}\\ \dot{\chi}\end{bmatrix} = \begin{bmatrix} g[(T-D)/W - \sin\gamma] \\ (g/V)(k_n n\cos\mu - \cos\gamma) \\ gk_n n\sin\mu/(V\cos\gamma)\end{bmatrix} + \boldsymbol{G}\boldsymbol{w} \quad (21)$$

where the drag is calculated by

$$D = 0.5\rho(V-V_w)^2SC_{D0} + 2kk_n^2n^2W^2/[\rho(V-V_w)^2S] \triangleq D_1 + D_2 \quad (22)$$

Here V, γ, and χ represent the airspeed, flight path angle, and heading angle respectively. The control variables are the applied thrust $T \le 113868.8N$, load factor $-1 \le n \le 2.66$, and bank angle $-25^o \le \mu \le 25^o$. The constants used in the model [32] are: wing area $S = 37.16m^2$, zero lift drag coefficient $C_{D0} = 0.02$, load factor effectiveness $k_n = 1$, induced drag coefficient $k = 0.1$, gravitational coefficient $g = 9.81kg/m^2$, atmospheric density $\rho = 1.2207kg/m^3$, and the weight of the selected UAV $W = 14515g$. To facilitate the control design, the drag has been separated into two parts $D_1 \triangleq 0.5\rho(V - V_w)^2 SC_{D0}$ and $D_2 \triangleq 2kk_n^2 n^2 W^2 / [\rho(V - V_w)^2 S]$, as shown in Eq. 22. The gust model $V_w = V_{w,n} + V_{w,t}$ is scaled based on [33], and varies according to the altitude z. In the simulated gust, the normal wind shear is given by

$$V_{w,n} = 0.215U \log_{10}(z) + 0.285U \tag{23}$$

where $U = 22.07\,m/s$ is the mean wind speed at an altitude of 5,000 meter. The turbulence part of the wind gust $V_{w,t}$ has a Gaussian distribution with a zero mean and a standard derivation of $0.09U$.

The first control objective is to track the desired output $V_d = 90\,m/s$, $\gamma_d = 5^o$, and $\chi_d = 1^o$ from the initial condition of $V_0 = 80\,m/s$, $\gamma_0 = 0^o$, and $\chi_0 = 0^o$. The second objective is to achieve desired stationary performance statistics of the state variables under two different noise levels. Here a quadratic form of the index is used as

$$J = \left[\sum_{i=1}^{3} \varpi_i (\mu_i - \mu_{i,d})^2 + \sum_{i=1}^{3} \vartheta_i (\sigma_i^2 - \sigma_{i,d}^2) \right]^{1/2} \tag{24}$$

where the mean μ_i, $i = 1,2,3$ and variance σ_i^2, $i = 1,2,3$ variables can be calculated from the moments (Eq. 16). The weights of the performance index, i.e. ϖ_i and ϑ_i, $i = 1,2,3$, are tuned to achieve a better convergence in NLP.

B. Uncertainty and Noise Models

The uncertainties and noise considered in the control design and simulation in Section E are described here. $\boldsymbol{w}(t) \in \Re^3$ (Eq. 21) is assumed to be a Weiner process with a zero-mean and a covariance matrix of $\boldsymbol{Q}(t)$, and the associated matrix $\boldsymbol{G}$ is assumed be identity as $\boldsymbol{I} \in \Re^{3\times 3}$. For the purpose of illustrating the capabilities of the algorithm, two noise settings are tried:

$$\text{Case 1: } \boldsymbol{Q} = diag([(0.25\,m/s^2)^2, (1^o/s)^2, (1^o/s)^2]) \tag{25}$$

$$\text{Case 2: } \boldsymbol{Q} = diag([(0.025\,m/s^2)^2, (0.1^o/s)^2, (0.1^o/s)^2]) \tag{26}$$

The control effectiveness of the thrust is assumed to be uniformly distributed as

$$T_a = (1 + \Delta_T) T_c \tag{27}$$

where T_c and T_a are the command and actual thrust respectively. The uncertainty Δ_T is uniformly distributed over $[-0.05, 0.05]$. The measurement noise in a typical speed indicator ΔV is assumed to be a Gaussian having a zero mean and $0.05\,m/s$ ($\approx \pm 0.1\,knot$) variance. Furthermore, a zero mean and 0.1^o variance Gaussian noise is assumed for both the flight path angle $\Delta\gamma$ and the heading angle $\Delta\chi$ measurements.

C. Nonlinear Robust Control Design

Rewrite the dynamics of the selected UAV (Eq. 21) in terms of Eq. (1) as

$$\dot{\boldsymbol{x}} = \boldsymbol{f}(\boldsymbol{x}) + \boldsymbol{B}(\boldsymbol{x})\boldsymbol{u} + \boldsymbol{G}\boldsymbol{w};\ \boldsymbol{y} = \boldsymbol{x} \tag{28}$$

in which

$$\boldsymbol{f}(\boldsymbol{x}) = [-g\sin\gamma - gD/W, -(g/V)\cos\gamma, 0]^T \tag{29}$$

$$\boldsymbol{B}(\boldsymbol{x}) = diag([g/W, k_n g/V, gk_n/(V\cos\gamma)]) \tag{30}$$

To handle the non-affine issue, a set of new control variables $\boldsymbol{u} \in \Re^{3\times 1}$ are introduced as $u_1 \triangleq T$, $u_2 \triangleq n\cos\mu$, and $u_3 \triangleq n\sin\mu$. Reversely, the actual control commands can be calculated by $\tan\mu = u_3/u_2$ and $n = \sqrt{u_2^2 + u_3^2}$. The nominal model used in the robust stochastic control design is

$$\dot{\boldsymbol{x}} = \hat{\boldsymbol{f}}(\boldsymbol{x}) + \hat{\boldsymbol{B}}(\boldsymbol{x})\boldsymbol{u} \tag{31}$$

where

$$\hat{\boldsymbol{f}}(\boldsymbol{x}) = [-g\sin\hat{\gamma} - g\hat{D}_1/W, -(g/\hat{V})\cos\hat{\gamma}, 0]^T \tag{32}$$

$$\hat{\boldsymbol{B}}(\boldsymbol{x}) = diag([g/W, k_n g/\hat{V}, gk_n/(\hat{V}\cos\hat{\gamma})]) \tag{33}$$

in which, $\hat{D}_1 = 0.5\rho\hat{V}^2 SC_{D0}$. The remaining part of the drag will be regarded as an uncertainty.

Based on Theorem 2, the controller has the following form

$$\boldsymbol{u} = \hat{\boldsymbol{B}}^{-1}\left[\frac{d\boldsymbol{y}_d}{dt} - \hat{\boldsymbol{f}}(\boldsymbol{x}) + \boldsymbol{k}\cdot\boldsymbol{s}\right] \tag{34}$$

and the sliding surface is $\boldsymbol{s} = \boldsymbol{y}_d - \boldsymbol{y}$ since the relative degree of the system is one (Eq. 18). To achieve the asymptotical stability, control parameters $\boldsymbol{k}$ need to satisfy

$$\boldsymbol{F} + \boldsymbol{D}\left|\frac{d\boldsymbol{y}_d}{dt} - \hat{\boldsymbol{f}}\right| + \boldsymbol{\eta}\cdot\boldsymbol{s} = (\boldsymbol{I} - \boldsymbol{D})\boldsymbol{k}\cdot\boldsymbol{s} \tag{35}$$

in which $\boldsymbol{\eta} > 0$, $\boldsymbol{\eta} \in \Re^{3\times 1}$ will be selected through the optimization to be discussed in Section D. Taking into account the uncertainties mentioned above, the functional uncertainty bounds $\boldsymbol{F} = [F_1, F_2, F_3]^T$ are derived as

$$F_1 = \left|\hat{f}_1 - f_1\right| \le g/W\left|D_1 - \hat{D}_1\right| + g/W\left|D_2\right| + g\left|\Delta\gamma\right| \tag{36}$$

$$F_2 = \left|\hat{f}_2 - f_2\right| \le (g/V_{\min})\Delta\gamma\left|\sin\gamma_{\max}\right| \tag{37}$$

and $F_3 = 0$, where

$$\left|(D_1 - \hat{D}_1)\right| \le 0.5\rho SC_{D0}(\Delta V^2 + V_{w,\max}^2 + 2\left|V_{\max}(\hat{V} - V_w)_{\max}\right| + 2\left|\Delta V V_{w,\max}\right|) \tag{38}$$

$$\left|D_2\right| \le 2kk_n^2 W^2 n_{\max}^2 / \left(\rho S\left|V_{\min} - V_{w,\max}\right|^2\right) \tag{39}$$

Here, the subscript "max" and "min" are used to denote the maximum and minimum values respectively. For example, in the simulation the speed of the UAV is assumed to be within $[80,120]\,m/s$, and the flight path angle is constrained by $\pm 10^o$. The uncertainty bound of the input matrix $\boldsymbol{D} = \text{diag}[D_{11}, D_{22}, D_{33}]$ are derived as $D_{11} = 0.05$,

$$D_{22} = k_n g\left|\left(\hat{V} - V\right)/\left(V\hat{V}\right)\right| \le k_n g\left(\left|\Delta V\right|\right)/V_{\min}^2 \tag{40}$$

$$D_{33} \le k_n g\left(\left|\Delta\gamma V_{\max}\sin\hat{\gamma} + \Delta V\Delta\gamma\sin\hat{\gamma}\right| + \left|\Delta V\right|\left|\cos\hat{\gamma}\right|\right)/\left(V_{\min}^2\cos^2\gamma_{\min}\right) \tag{41}$$

when $\Delta\gamma$ is small.

D. Stochastic Control Design

With the control law defined as shown in Eqs. 34 through 41, the closed-loop system can be converted to the following Itô form as

$$d\boldsymbol{x} = \boldsymbol{f}'(\boldsymbol{x},\boldsymbol{\eta})dt + \boldsymbol{G}d\boldsymbol{\beta}(t) \tag{42}$$

where $\boldsymbol{f}'(\boldsymbol{x},\boldsymbol{\eta}) = \boldsymbol{f}(\boldsymbol{x}) + \boldsymbol{B}\hat{\boldsymbol{B}}^{-1}\left[dy_d/dt - \hat{\boldsymbol{f}}(\boldsymbol{x}) + \boldsymbol{k}\cdot\boldsymbol{s}\right]$ and $\boldsymbol{k}\cdot\boldsymbol{s}$ is a function of the control parameter $\boldsymbol{\eta} > 0$. Note that $d\boldsymbol{\beta}(t) \sim \boldsymbol{w}(t)dt$. The corresponding FPE that governs the state PDF $p(\boldsymbol{x})$ is derived as

$$\frac{\partial p}{\partial t} = -\sum_{i=1}^{3}\frac{\partial\left[pf_i'\right]}{\partial x_i} + \sum_{i=1}^{3}\sum_{j=1}^{3}\frac{\partial^2\left[p\left(\boldsymbol{D}(\boldsymbol{x})\right)_{ij}\right]}{\partial x_i \partial x_j} \tag{43}$$

where $\boldsymbol{D} = 1/2\boldsymbol{GQG}^T$. In this example, the state PDF is approximated through the DQMOM approach as

$$p(\boldsymbol{x}) = \sum_{\alpha=1}^{N} w_\alpha(t)\prod_{j=1}^{3}\delta[x_j - \langle x_j\rangle_\alpha] \tag{44}$$

and the k_1, k_2, k_3 moments of the state PDF is derived as

$$M^{k_1k_2k_3} \triangleq \left\langle x_1^{k_1}, x_2^{k_2}, x_3^{k_3}\right\rangle = \sum_{\alpha=1}^{N} w_\alpha \prod_{j=1}^{3}\langle x_j\rangle_\alpha^{k_j} \tag{45}$$

E. Simulation Settings and Results

The moment constraints in Eq. (11) are carefully selected for the case of $N = 4$ after trials and errors. In this moment description, for example, the first column $[1,0,0]^T$ gives the mean value of the speed, whereas seventh column $[1,1,0]^T$ presents the covariance of the speed and the flight path angle. The MATLAB® function fminsearch is used for the NLP optimization to find the proper control parameter $\boldsymbol{\eta}$. The Euler-Maruyama scheme [34] is used in the propagation of the SDE (Eq. 42). The found control parameters are tested in four thousand Monte Carlo runs, and compared with the case where arbitrarily selected parameter $\boldsymbol{\eta} = [1,1,1]^T$ is used, i.e. without the offline stochastic optimization. To simplify the description, the proposed stochastic robust controller is denoted as "method 1", whereas the nonlinear robust controller method using arbitrarily selected control parameters is represented as "method 2". Note that the uncertainties and noise mentioned in Section B are applied in the Monte Carlo simulation to show the robustness of the algorithm.

It can be seen in Figs. 1-6 that the mean values of the speed (V), flight path angle (γ), and heading angle (χ) are successfully controlled with relatively small steady state errors in both methods except in the speed histories in Figs. 1 and 2. Under the two different noise simulations, the mean values of the speed achieved by method 1 are 89.64 and 89.45 respectively, whereas those of method 2 are 88.71 and 88.80 respectively. Therefore, in terms of controlling the mean value of the states, there are no significant differences between method 2 and the proposed method 1 since both methods are asymptotically stable in tracking.

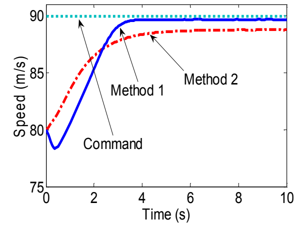

Fig. 1 Speed mean value (Case 1)

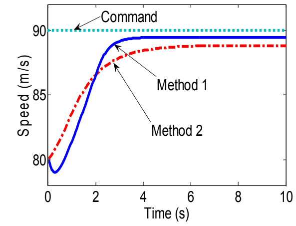

Fig. 2 Speed mean value (Case 2)

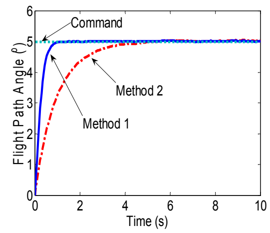

Fig. 3 Mean value of γ (Case 1)

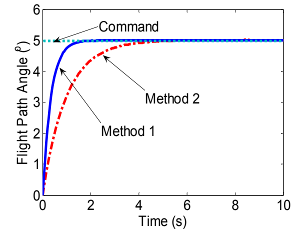

Fig. 4 Mean value of γ (Case 2)

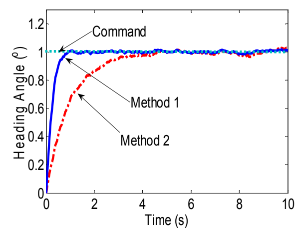

Fig. 5 Mean value of χ (Case 1)

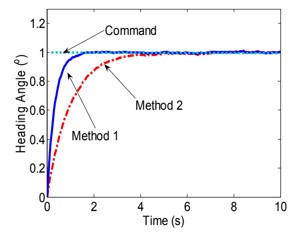

Fig. 6 Mean value of χ (Case 2)

The significance and advantage of method 1 can be easily seen from Figs. 7-10, as well, method 1 has successfully controlled the variances $\sigma_{V,a}^2$, $\sigma_{\gamma,a}^2$, and $\sigma_{\chi,a}^2$ very closely toward the desired values as 0.095, 0.255, and 0.26 in case 1. Notice that the units are intentionally neglected for a convenient description here. However, in method 2, the stationary variance values are 0.36 (Fig. 7), 1.04 (Fig. 9), and 1.05 (Fig. 9) respectively, which are far away from the desired statistic (0.1, 0.25, and 0.25 respectively). The same conclusion can be made in case 2, as shown in Figs. 8 and 10. Furthermore, as shown in Figs. 7 and 8, the relatively larger magnitude shown in the first part of speed variance represents a wider distribution of the speed performance in the Monte Carlo simulation, which doesn't mean a relatively larger transient performance.

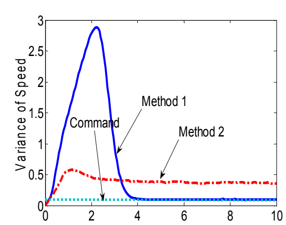

Fig. 7 Speed variance (Case 1)

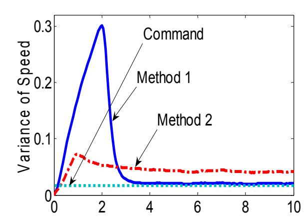

Fig. 8 Speed variance (Case 2)

Furthermore, the stationary mean and variance values found from the optimization match well with the Monte Carlo simulation. For example, the desired variance of the heading angle in Case 1 is $\sigma_{\chi,d}^2 = 0.25$, the achieved variance in the optimization is $\sigma^2_{\chi,o} = 0.25$, whereas when the control parameters obtained in the optimization is used in the Monte Carlo simulation, the achieved variance is $\sigma^2_{\chi,a} = 0.26$.

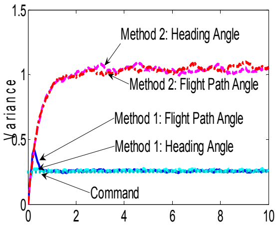

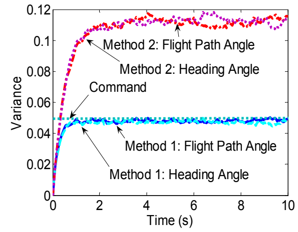

Fig. 9 Variance of γ and χ (Case 1) **Fig. 10** Variance of γ and χ (Case 2)

VII. Conclusion

In this paper, a novel approach based upon the direct quadrature method of moments is proposed for nonlinear systems subject to parametric and functional uncertainties with random excitations. The proposed nonlinear feedback controller is robust with respect to parametric and functional uncertainties without discontinuous functions involved, which is preferred by the associated Fokker Planck Equation. The advantages of the method are (1) it is able to control the distribution of any specified stationary moments of the states/output probability density function (PDF), (2) the method is of interest because the process is not necessary a Gaussian, and (3) the controller is robust with respect to parametric and functional uncertainties without involving discontinuous functions. A non-trivial UAV tracking problem has demonstrated the capability of the proposed nonlinear stochastic control method.

References

[1] Wang, Q., and Stengel, R. F., "Probabilistic control of nonlinear uncertain systems," *Probabilistic and Randomized Methods for Design under Uncertainty*, Springer-Verlag, London, 2006, pp. 381-414.

[2] Oshman, Y., "Linear quadratic stochastic control using the singular value decomposition," *J. Guid. Control Dyn.*, Vol. 15, No. 4, 1992.

[3] Iwasaki, T., and Skelton, R. E., "On the observer-based structure of covariance controllers," *Syst.Control Lett.*, Vol. 22, 1994, pp. 17-25.

[4] Lewis, A. S., and Sinha, A., "Sliding Mode Control of Mechanical Systems with Bounded Disturbances via Output Feedback," *J. Guid. Control Dyn.*, Vol. 22, No. 2, March-April 1999, pp. 235-240.

[5] Grigoriadis, K. M., and Skelton, R. E., "Minimum-energy covariance controllers," *Automatica*, Vol. 33, 1997, pp. 569-578.

[6] Bratus, A., Dimentberg, M., and Iourtchenko, D., "Optimal bounded response control for a second-order system under a white-noise excitation," *Journal of Vib. and Control*, Vol. 6, 2000, pp. 741–755.

[7] Hotz, A., and Skelton, R. E., "Covariance control theory," *International Journal of Control*, Vol. 46, No. 1, 1987, pp. 13-32.

[8] Hu, G., Lou, Y., and Christofides, P. D., "Dynamic output feedback covariance control of linear stochastic dissipative partial differential equations," *American Control Conf.*, Seattle, June 2008, pp. 260-266.

[9] Lou, Y., and Christofides, P. D., "Nonlinear feedback control of surface roughness using a stochastic PDE," *45th IEEE Conference on Decision and Control*, San Diego, CA, Dec., 2006, pp. 936-943.

[10] Young, G. E., and Chang, R. J., "Optimal control of stochastic parametrically and externally excited nonlinear control systems," *ASME Journal of Dyn. Syst., Meas., and Control*, Vol. 110, 1988, pp. 114-119.

[11] Wojtkiewicz, S. F., and Bergman, L. A., "A moment specification algorithm for control of nonlinear system driven by Gaussian white noise," *Nonlinear Dyn.*, Vol. 24, No. 1, 2001, pp. 17-30.

[12] Jazwinski, A., *Stochastic process and filtering theory*, New York, NY, Academic Press, 2007 pp. 72-74.

[13] Daum, F., "Nonlinear filters: beyond the kalman filter," *IEEE Aerospace and Electronic Systems Magazine*, Vol. 20, No. 8, 2005.

[14] Naess, A., and Johnson J. M., "Response statistics of nonlinear dynamics systems by path integration," *the Proceeding of IUTAM Symposium on Nonlinear Stochastic Mechanics*, 1992, pp. 401–414.

[15] Sun J. Q., and Hsu C. S., "The generalized cell mapping method in nonlinear random vibration based upon short-time gaussian approximation," *ASME Journal of Applied Mechanic*, Vol. 57, 1990.

[16] Challa, S., and Bar-Shalom, Y., "Nonlinear filter design using fokker-planck-kolmogorov probability density evolutions," *IEEE Trans. on Aero. and Electr. Syst.*, Vol. 36, No. 1, 2000, pp. 309-315.

[17] Yoon, J., and Xu, Y., "Relative position estimation using fokker-planck and Bayes' equations," *AIAA Guid., Navigation, and Control Conference and Exhibit*, Aug. 2007, Hilton Head, South Carolina.

[18] Sun, J. Q., and Hsu, C. S., "Cumulant-neglect closure method for asymmetric nonlinear systems driven by Gaussian white noise," *Journal of Sound and Vibration*, Vol. 135, 1989, pp. 338-345.

[19] Sobczy, K., and Trebicki, J., "Maximum entropy principle in stochastic dynamics," *Prob. Eng. Mechanics*, Vol. 3, No. 5, 1990, pp. 102-110.

[20] Chang, K. Y., Wang, W. J., and Chang, W. J., "Constrained control for stochastic multivariable systems with hysteresis nonlinearity," *International Journal of Syst. Sci.*, Vol. 28, No. 7, 1997, pp. 731-736.

[21] Kim, J., and Rock, S., "Stochastic feedback controller design considering the dual effect," *AIAA Guid., Navigation, and Control Conference and Exhibit,* Aug. 2006, Keystone, Colorado.

[22] Forbes, M. G., Forbes, J. F., and Guay, M., "Regulatory control design for stochastic processes: shaping the probability density function," *2003 American Control Conf.*, Denver, Colorado June 2003, pp. 3998-4003.

[23] Su, Q., and Strunz, K., "Stochastic polynomial-chaos-based average model of twelve-pulse diode rectifier for aircraft applications," *IEEE Compel. Work. on Comp. in Power Electron.*, Troy, NY, July 2006.

[24] Yue, H., and Wang, H., "Minimum entropy control of closed-loop tracking errors for dynamic stochastic systems," *IEEE Trans. Autom. Control*,, Vol. 48, No. 1, Jan. 2003, pp. 118-122.

[25] Kumar, M., Chakravorty, S., and Junkins, J. L., "Computational nonlinear stochastic control based on the fokker-planck-kolmogorov equation," *AIAA Guid., Navigation, and Control Conference and Exhibit*, Aug. 2008, Honolulu, Hawaii.

[26] Utkin, V. I., "Variable structure systems with sliding modes," *IEEE Trans. Autom. Control*,, Vol. 22, No. 2, April 1977, pp. 212-222.

[27] Bartolini, G., Ferrara, A., Usai, E., and Utkin, V. I., "On multi-input chattering-free second order sliding mode control," *IEEE Trans. Autom. Control*,, Vol. 45, No. 9, September 2000, pp. 1711-1717.

[28] Slotine, J. E., and Li, W., *Applied nonlinear control*, New Jersey: Prentice Hall, 1990, pp. 267-307.

[29] Buffington, J. M., and Shtessel, Y. B., "Saturation protection for feedback linearizable systems using sliding mode theory," *1998 American Control Conference*, Philadelphia, PA, 1998, pp. 1028-1032.

[30] Kokotovic, P., Khalil, H. K., and O'Reilly, J., *Singular perturbation methods in control, analysis and design*, Society for Industrial and Applied Mathematics, Philadelphia, 1999, pp. 1-45.

[31] Hopkins, R., and Xu, Y., "Position tracking control for a simulated miniature helicopter," *AIAA Guid,, Navigation, and Control Conference and Exhibit*, Aug. 2008, Honolulu, Hawaii.

[32] Unnikrishnam, N. and Balakrishnan, S. N., "Neuroadaptive model following controller design for a nonaffine UAV model," *2006 American Control Conf.*, Minneapolis, Minnesota, USA, June 2006.

[33] AC 120-28D: List of Appendices – Appendix 4: Wind model for approach and landing simulation.

[34] Kloeden, P. E., and Platen, E., *Numerical solution of stochastic differential equations*, Springer-Verlag, Berlin, 1992, pp. 340-344.

[35] Marchisio, D. L., and Fox, R. O, "Solution of population balance equations using the direct quadrature method of moments" *Journal of Aerosol Science*, Vol. 36, 2005, pp. 43-73.